

Phase-Modulated Radar Waveform Classification Using Deep Networks

Michael Wharton, Anne M. Pavy, and Philip Schniter

Abstract—We consider the problem of classifying noisy, phase-modulated radar waveforms. While traditionally this has been accomplished by applying classical machine-learning algorithms on hand-crafted features, it has recently been shown that better performance can be attained by training deep neural networks (DNNs) to classify raw I/Q waveforms. However, existing DNNs assume time-synchronized waveforms and do not exploit complex-valued signal structure, and many aspects of their DNN design and training are suboptimal. We demonstrate that, with an improved DNN architecture and training procedure, it is possible to reduce classification error from 18% to 0.14% on asynchronous waveforms from the SIDLE dataset. Unlike past work, we furthermore demonstrate that accurate classification of multiple overlapping waveforms is also possible, by achieving 4.0% error with 4 asynchronous SIDLE waveforms.

I. INTRODUCTION

We consider the problem of classifying phase-modulated radar waveforms given raw signal data. Waveform classification is an important capability for cognitive radar. To train a classifier, we assume the availability of a dataset containing many examples of radar waveforms (i.e., sequences of complex-valued time-domain samples) with corresponding class labels in $\{1, \dots, K\}$. In this work, we focus on deep neural network (DNN) classifiers, as they are state-of-the-art.

Several challenges are faced when designing DNN classifiers of raw radar waveforms, commonly referred to as “pulses.” First, the pulse duration can span a very wide range (e.g., from hundreds to thousands of samples) even within a given class. Most DNNs, however, assume a fixed input dimension. Second, the pulses are complex-valued, whereas most DNNs are configured to support real-valued signals. Third, when applying the classifier, one cannot assume that the pulse will be time-synchronized, especially in passive sensing applications. Fourth, practical radar systems must operate over a wide range of signal-to-noise ratios (SNRs), including SNRs far below 0 dB. To be practical, all of these challenges must be simultaneously addressed.

Early approaches to radar waveform classification first converted the raw waveforms to hand-crafted, low-dimensional features, to which classic machine-learning techniques could be applied. For example, [1] designed auto-correlation function (ACF) features of dimension 20 that were robust to time and frequency shifts, and trained a Fisher’s linear discriminant

classifier. These ACF features were later used in [2] with a support vector machine (SVM) classifier and in [3] with a shallow neural-network classifier.

It was recently demonstrated in [3] that significantly better classification accuracy could be obtained by training a DNN to operate on raw time-domain radar waveforms. This is not surprising, since the early DNN layers can learn a feature representation that outperforms hand-crafted ones, which is then classified by the final DNN layers.

Still, several assumptions were made in [3] that limited both the performance and practicality of the methodology. First, the DNN input dimension in [3] was chosen to be greater than the longest pulse in the training dataset. We will show that it is better to truncate or pad the pulses to an optimized input length. Second, the DNN in [3] ignored the quadrature (Q) input to avoid complex-valued operations. We show that a well-designed complex-valued DNN has advantages over a real-valued DNN. Third, the training and test waveforms in [3] were assumed to be time-synchronized, which is impractical. We train our DNN to be robust to time-asynchronous inputs. Fourth, the DNN architecture in [3] is far from optimal. We make an effort to optimize our DNN architecture (e.g., input dimension, depth, width, kernel size) and training procedure (e.g., batch size, learning rate). Additionally, we use data augmentation (i.e., random noise and delay realizations) to effectively increase the size of the training dataset. Fifth, [3] assumed a single radar pulse, whereas we also consider the problem of classifying multiple overlapping radar pulses.

II. APPROACH

A. Network Architecture

Like in [3], we focus on feed-forward convolutional DNNs. (Although we experimented with recursive networks, our initial results were not competitive.) In particular, we focus on deep residual networks (ResNets) [4] due to their excellent performance on related tasks. Although ResNets were originally proposed for classification of images, they can be easily adapted to one-dimensional signals by changing the two-dimensional convolutions to one-dimensional convolutions and appropriately modifying the kernel sizes and numbers-of-channels.

For single-pulse classification, we train with the standard cross-entropy (CE) loss. For multi-pulse classification, we use the same network architecture, but train using binary cross-entropy (BCE) loss on each of the K outputs.

M. Wharton and P. Schniter are with the Dept. of ECE, The Ohio State University, Columbus OH 43210 (email: wharton.124@buckeyemail.osu.edu; schniter.1@osu.edu). A. M. Pavy is with the Sensors Directorate, Air Force Research Lab, WPAFB, OH, 45433 (email: anne.pavy@us.af.mil).

This work was funded in part by the National Science Foundation under Grant 1539961.

B. Complex Arithmetic

Most DNNs support only real-valued arithmetic, which is sufficient when the data is real-valued. But our radar waveforms are complex-valued. The question is then how to best handle these complex waveforms.

Many approaches have been proposed to handle complex-valued signals with real-valued DNNs. Whether or not they are successful or not depends largely on the application. One of the simplest approaches is to feed the magnitude of the complex-valued signal to the DNN. Although this was successfully used in [5] to classify synthetic aperture radar (SAR) images, we found that it did not work well for classification of phase-modulated radar waveforms. Another simple approach is to feed only the real part of the complex-valued signal to the DNN. Although was successfully used in [3] to classify phase-modulated radar waveforms, we show in the sequel that it can be improved upon. Another approach is to stack the real and imaginary parts of the waveform into a real-valued 2-row “image” and feed it to a real-valued DNN with 2-dimensional convolutions [6]. Yet another approach is to feed the real and imaginary components into two separate input channels of a real-valued DNN, similar to how RGB image data is typically fed into three separate input channels.

An alternative is to design a complex-valued DNN. Such networks have led to improved performance in, e.g., audio classification [7] and magnetic resonance image (MRI) reconstruction [8] tasks. To understand what we mean by a “complex-valued DNN,” consider the multiplication of a learnable parameter $k = k_r + ik_i \in \mathbb{C}$ with a feature $x = x_r + ix_i \in \mathbb{C}$, where $k_r, x_r \in \mathbb{R}$ represent real parts, $k_i, x_i \in \mathbb{R}$ represent imaginary parts, and $i \triangleq \sqrt{-1}$. Such multiplications arise in DNNs when implementing convolution and when linearly combining the convolution outputs. The complex-valued multiplication of k and x can be written using four real-valued multiplications as

$$kx = (k_r x_r - k_i x_i) + i(k_i x_r + k_r x_i). \quad (1)$$

The key point is that (1) is a two-input/two-output operation with only two learnable parameters: $k_r, k_i \in \mathbb{R}$. By contrast, a 2-channel real-valued DNN would implement

$$y_1 = k_{11}x_1 + k_{12}x_2 \quad (2)$$

$$y_2 = k_{21}x_1 + k_{22}x_2, \quad (3)$$

with $x_1 \triangleq x_r$ and $x_2 \triangleq x_i$, which involves four learnable parameters: $k_{11}, k_{12}, k_{21}, k_{22} \in \mathbb{R}$. Reducing the number of learnable parameters helps to mitigate overfitting.

With regards to the construction of complex-valued activation functions (which are essentially two-input/two-output memoryless nonlinearities), there are many options, as discussed in [7], [8]. Since both papers suggest that

$$\text{CReLU}(x) \triangleq \max\{0, x_r\} + i \max\{0, x_i\} \quad (4)$$

for $x = x_r + ix_i$

outperforms other complex-valued activations in many applications, we use (4) in our network.

Complex-valued implementations of batch-norm have also been developed (see, e.g., [8]). In our implementation, for

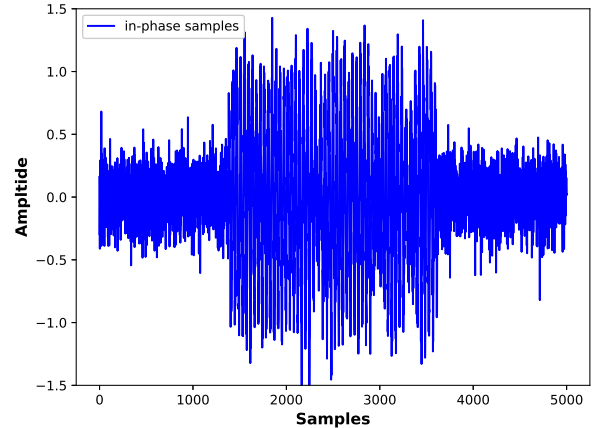


Fig. 1. Example synchronous noise-padded waveform at SNR=10.8dB, waveform length $N = 2261$, and DNN input length $D = 5000$.

simplicity, we apply standard batch-norm separately to the real and imaginary outputs.

C. Noise Padding / Truncation / Delay

As mentioned earlier, our raw radar waveforms differ in duration from hundreds to thousands of samples, even within a single class. However, the ResNet DNN forces us to choose a fixed input dimension for minibatch training. The usual approach (e.g., routinely used in image classification) is to set the input dimension equal to the longest samples (e.g., largest images) and zero-pad the shorter samples as needed.

With noisy radar waveforms, it would be more appropriate to noise-pad rather than zero-pad. Thus, in [3], the waveforms were symmetrically padded with white Gaussian noise whose variance was selected to match the noise content of the original sample. An example is shown in Fig. 1.

There are several issues with the approach from [3]. First, as a consequence of symmetric padding, the padded waveforms will all be time-centered, i.e., synchronized. But since time synchronization is not expected in practice, it is not advantageous to train on time-synchronized waveforms. Second, noise-padding reduces SNR. In particular, if a sample is $P \times$ longer after noise-padding, then its SNR will change by the factor $1/P$. Third, the approach in [3] was to pad each training sample with a *fixed* noise waveform. In this case, the DNN could attempt to classify based on this noise realization, which leads to overfitting. This latter problem is exacerbated by the very low SNRs encountered in radar.

Our approach is to noise-pad *or* truncate the training waveforms as needed to obtain a fixed input length of D , where D is optimized. This approach recognizes that noise-padding decreases SNR, while truncation discards discriminative features, and so the optimal approach must balance between these extremes. To avoid injecting time-synchronization bias into the training procedure, we randomly delay the training waveform whenever noise-padding or truncating that waveform. We can describe this more precisely using N to denote the duration of the original training waveform and U to denote a random integer uniformly distributed from 0 and $|N - D|$. When $N < D$, we noise-pad the front of the waveform using

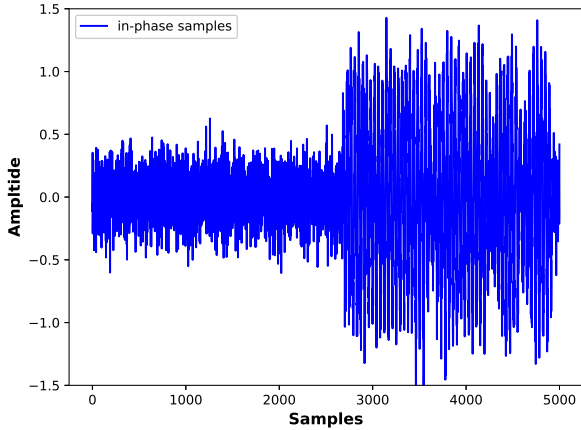


Fig. 2. Example asynchronous noise-padded waveform at SNR=10.8dB, waveform length $N = 2261$, DNN input length $D = 5000$, delay $U = 2700$.

U samples and noise-pad the back of the waveform using $D - N - U$ samples. (See Fig. 2.) When $N > D$, we keep D consecutive samples of the training waveform starting at index U . To avoid (over)fitting the DNN to particular training noise waveforms or training delays U , we draw new realizations of these quantities in every training minibatch (e.g., in the DataLoader of PyTorch [9]). This approach can be recognized as a form of “data augmentation” [10] that increases the effective number of the training samples. Finally, we optimized the input dimension D over a grid of possibilities, as described in the sequel.

III. EXPERIMENTAL RESULTS

For our experiments, we use the SIDLE dataset, which was also used in [1]–[3]. This dataset contains 23 classes of phase-modulated radar pulses with 10000 examples of single pulses from each class. For a fair comparison to [3], we omitted classes 6 and 19–23 in the original dataset and used only the remaining $K = 17$ classes to train and test our DNN. For these 17 classes, the dataset contains complex-valued waveforms with lengths from between 131 and 8925 samples and SNRs between -12 and $+12$ dB. For each experiment, we used a random subset of 80% of the dataset for training and the remaining 20% for testing. We used the Adam optimizer with default parameters $\beta_1 = 0.9$ and $\beta_2 = 0.999$. In what follows, we discuss classification of single pulses in Sections III-A and III-B and multiple pulses in Section III-C.

A. Baseline

As a baseline, we first investigate the performance of the 9-layer real-valued convolutional DNN from [3] on the task of single-pulse classification. As described earlier, this network uses an input dimension of 11000 and discards the imaginary part of the input. To train the network, we used the synchronous noise-padding approach described in Section II-C and illustrated in Fig. 1, and saw that the network converged to 0% training error. We then tested the network using synchronous noise-padded data from the test set, and observed 3.57% test error, similar to what was reported in [3].

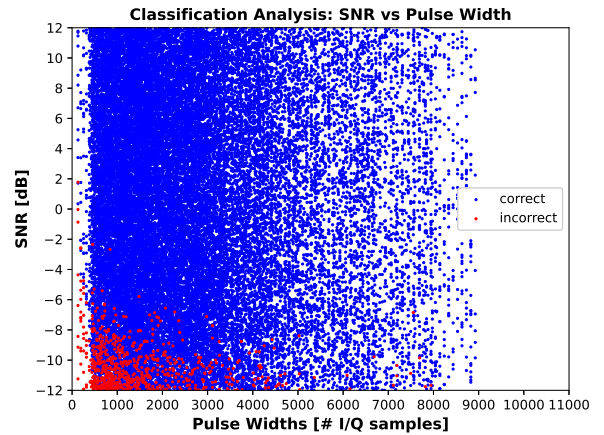


Fig. 3. Classification outcome (true=blue, false=red) of 11000-input ResNet-30 vs. pre-padded SNR and pulse length.

Next, to evaluate how well this DNN performs in the practical asynchronous setting, we re-trained it using the asynchronous noise-padding approach proposed in Section II-C and illustrated in Fig. 2. When testing with similarly processed (i.e., asynchronous) test data, we observed a test error of 18.29%. This relatively poor performance motivates the design of an improved DNN for asynchronous single-pulse classification.

B. Improvements

ResNet: As a first step, we swap the DNN from [3] with a 30-layer ResNet, but still use input dimension 11000 and only the real part of the radar waveform. We configured the ResNet using PyTorch’s default parameters, but with a one-dimensional kernel rather than a two-dimensional kernel. Training and testing this ResNet-30 using the asynchronous noise-padding approach from Section II-C gave 2.14% test error, which significantly improves upon the 9-layer DNN from [3].

Optimized input-length: To better understand how we might be able to improve the ResNet performance, we plot the classification outcome (i.e., correct or incorrect) versus pre-padded waveform length and SNR in Fig. 3. The figure shows that pulses with both short length and low SNR are most likely to be misclassified. This is consistent with the discussion in Section II-C, which described how noise-padding by factor P causes the SNR to change by the factor $1/P$. Thus, when the network input dimension is very large, short pulses will suffer a large SNR reduction that, when combined with an already low SNR, will likely result in misclassification.

To circumvent this problem, we allow smaller network input dimension D and either truncate or noise-pad each N -length raw waveform as needed (as described in Section II-C). Table I reports test error rate for several values of D . The table shows that $D = 3317$ was best among the tested values for the ResNet-30. As a consequence of this D -optimization, the test error improved from 2.14% to 1.32%.

Complex-valued DNN: To improve the DNN further, we incorporate the complex-valued operations from Section II-B

TABLE I
RESNET-30 VS. INPUT LENGTH

Input Length	1000	1821	3317	6040	11000
Test Error	8.50%	2.16%	1.32%	1.35%	2.14%

TABLE II
RESNET-30 VS. CRESNET-30

Model	Test Error	Trainable Parameters
ResNet-30	1.52%	1782193
IQ-ResNet-30	0.39%	1782417
CResNet-30	0.36%	1690189

TABLE III
FINE-TUNED CRESNET RESULTS VS. NETWORK DEPTH

Model	Test Error	# Parameters	Width	Kernel
CResNet-22	0.16%	7721041	32	11
CResNet-26	0.16%	1818161	16	7
CResNet-30	0.14%	659233	8	9
CResNet-34	0.15%	670945	8	9
CResNet-38	0.16%	2228913	16	7

in the ResNet and refer to it as the ‘‘CResNet.’’ We also show results for the real-valued DNN utilizing both in-phase and quadrature radar waveform data from (3), which we call the ‘‘IQ-ResNet.’’ For a fair comparison, we adjusted the number of channels in the CResNet-30 and the IQ-ResNet-30 so that the number of trainable parameters is approximately equal to that in the (real-valued) ResNet-30. The resulting test error rates are shown in Table II for input length 3317, which shows the improvement brought by the CResNet.

Network Fine-Tuning: As a final step, we performed an extensive fine-tuning of the CResNet. This included a simultaneous search over network depth, network width, kernel width, batch size, and learning rate. For network and kernel width, we adjusted the 1st and 2nd layers respectively, and scaled the remaining layers in the same way as done in the default ResNets in PyTorch. The test error (averaged over 100 random delays and noise realizations) and # of trainable parameters for the optimized network and kernel widths of the fine-tuned CResNet are given in Table III. A batch size of 512, learning rate of 0.001, and first-layer kernel width of 11 sufficed for all widths and depths. Each network was trained for 90 epochs, but stopped early if the test loss did not improve for 15 consecutive epochs. In the end, with fine-tuning, the test error rate dropped to 0.14%.

C. Classification of multiple overlapping pulses

We now use the fine-tuned network architecture to classify multiple overlapping pulses. For this purpose, we retrained the network to minimize binary cross-entropy (BCE) loss on each of the $K = 17$ outputs, rather than cross-entropy (CE) loss. The resulting network outputs a real-valued vector for which a positive entry in the k th location indicates that a pulse from the k th class is believed to be present, while a negative entry indicates that no pulse is believed to be present.

Our experiments consider $L \in \{1, 2, 3, 4\}$ simultaneously overlapping waveforms. For a given L , multi-pulse waveforms were generated by first creating one asynchronous noise-padded waveform (as described in Section II-C) and then

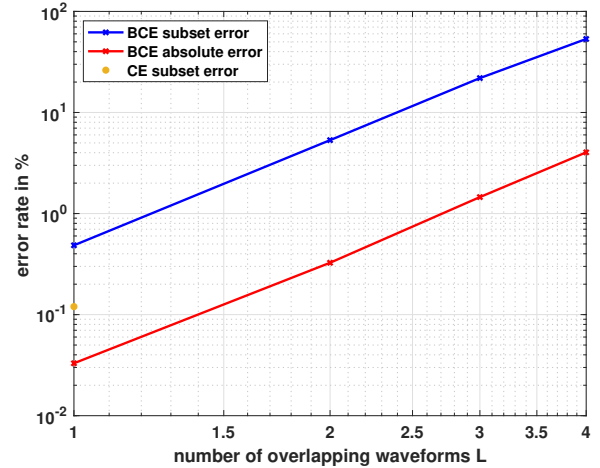


Fig. 4. Subset and absolute error-rate versus number of simultaneously overlapping waveforms L for the BCE-trained and CE-trained networks.

adding $L - 1$ additional asynchronous noiseless zero-padded waveforms. This way, the SNRs of the multi-pulse waveforms remained between -12 and $+12$ dB. A single network was trained by sampled L uniformly over $\{1, 2, 3, 4\}$.

There are two common ways to define the error-rate of multi-label classification: ‘‘absolute error’’ (E_{abs}) refers to the error on the binary predictions, whereas ‘‘subset error’’ (E_{sub}) refers to the error on the K -ary prediction vector as a whole. If the binary prediction errors are i.i.d., then $E_{\text{sub}} = 1 - (1 - E_{\text{abs}})^K \approx KE_{\text{abs}}$ using the binomial approximation, which is accurate for small E_{abs} .

Our test error-rate results for fixed $L \in \{1, 2, 3, 4\}$ overlapping pulses (using an 80/20% training/testing split) are presented in Fig. 4. There we see that both $\log E_{\text{abs}}$ and $\log E_{\text{sub}}$ grow approximately linearly with $\log L$. We also see that $E_{\text{sub}} \approx KE_{\text{abs}}$. Furthermore, we see that the single-pulse network (from Section III-B) outperformed the multipulse network in the special case of $L=1$ test pulses, but this is not surprising because it was trained for this special case. Still, with 4 overlapping pulses, the multi- L network achieves an absolute error of only 4.0%.

IV. CONCLUSION

In this work, we considered the classification of phase-modulated radar waveforms given raw complex-valued signal data. For this purpose, we designed a complex-valued ResNet with optimized parameters, including width, depth, kernel width, batch size, and learning rate. We also optimized the input dimension, necessitating either waveform truncation or noise-padding (as appropriate). Our training procedure used random delays, random noise waveforms, and a wide range of SNRs for robustness and to avoid overfitting. After fine-tuning, our network achieved a test error of 0.14% on single-pulse classification of asynchronous SIDLE data, which is a significant improvement over the previous state-of-the-art approach [3], which achieved 18.29%. When trained for multi-pulse classification, our network obtained an absolute error of 4.0% with 4 overlapping pulses. For future work, it would be interesting to investigate alternative architectures such as the DenseNet [11].

REFERENCES

- [1] B. Rigling and C. Roush, "ACF-Based classification of phase modulated waveforms," in *Proc. IEEE Radar Conf.*, pp. 287–291, 2010.
- [2] A. Pavy and B. Rigling, "Phase modulated radar waveform classification using quantile one-class SVMs," in *Proc. IEEE Radar Conf.*, pp. 745–750, 2015.
- [3] R. V. Chakravarthy, H. Liu, and A. M. Pavy, "Open-set radar waveform classification: Comparison of different features and classifiers," in *Proc. IEEE Radar Conf.*, pp. 542–547, 2020.
- [4] K. He, X. Zhang, S. Ren, and J. Sun, "Deep residual learning for image recognition," in *Proc. IEEE Conf. Comp. Vision Pattern Recog.*, pp. 770–778, 2016.
- [5] M. Wharton, E. T. Reehorst, and P. Schniter, "Compressive SAR image recovery and classification via CNNs," in *Proc. Asilomar Conf. Signals Syst. Comput.*, pp. 1081–1085, 2019.
- [6] T. J. O'Shea, J. Corgan, and T. C. Clancy, "Convolutional radio modulation recognition networks," in *Prof. Intl. Conf. Eng. Appl. Neural Netw.*, pp. 213–226, 2016.
- [7] C. Trabelsi, O. Bilaniuk, Y. Zhang, D. Serdyuk, S. Subramanian, J. F. Santos, S. Mehri, N. Rostamzadeh, Y. Bengio, and C. J. Pal, "Deep complex networks," in *Proc. Internat. Conf. on Learning Repres.*, 2018.
- [8] E. K. Cole, J. Y. Cheng, J. M. Pauly, and S. S. Vasanawala, "Analysis of deep complex-valued convolutional neural networks for MRI reconstruction," *arXiv:2004.01738*, 2020.
- [9] E. Stevens, L. Antiga, and T. Viehmann, *Deep Learning with PyTorch*. Shelter Island, NY: Manning, 2020.
- [10] I. Goodfellow, Y. Bengio, and A. Courville, *Deep Learning*. MIT Press, 2016.
- [11] G. Huang, Z. Liu, L. Van Der Maaten, and K. Q. Weinberger, "Densely connected convolutional networks," in *Proc. IEEE Conf. Comp. Vision Pattern Recog.*, pp. 4700–4708, 2017.